MODIFICATION OF OXIDATION BEHAVIOR OF Ni Ti SHAPE-MEMORY ALLOY BY YTTRIUM ADDITION

NAWAL MOHAMMED DAWOOD & OSAMAH IHSAN ALI

Department of Metallurgical Engineering, College of Materials Engineering, Babylon University, Babil, Iraq

Original Article

ABSTRACT

The current research studies the influences of adding yttrium element on the oxidation behavior of NiTi- Shape Memory Alloy system (SMAs). Specimens were manufactured by powder technology method, the blended powder consisting of titanium and nickel with constituents of (45 %wt.) and (55% wt.) correspondingly. Yttrium was added in different weight percentage of (0.5 and 0.9). The constituents of powders were blended for five hours and later compressed with stable compressing load of (800) MPa to cylinder-shaped specimens. Sintering procedure done at a specific temperature (950 °C for 6 hours) in vacuum circumstances (10^{-4}) torr. Later, the specimens cool down in vacuum condition till room temperature. The outcomes of X-ray diffraction analysis revealed that entirely specimens (without and with additions) contained [NiTi (B19) and (NiTi (B2)]. Periodic oxidation tests were performed in static air at temperatures (800, 900, and 1000°C) for 100 hrs and 10 hours per period to evaluate the behavior of oxidation for all specimens. The results showed that the behavior of oxidation of NiTi (without and with additives) were subjected to parabolic law. Further, the performance of NiTi SMAs was modified after yttrium addition. For the base NiTi alloy, the parabolic rate constant (kP) differs from akP = 2.4502×10^{-7} ($mg^2/cm^4.s$) at 800 °C to a specific value of kP = 10.609×10^{-7} ($mg^2/cm^4.s$) at 1000 °C, and the activation energy (Q=297 kJ/mol), while NiTi 0.5 wt.% Y alloy, the (Kp) varies from a Kp = 0.531×10^{-7} ($mg^2/cm^4.s$) at 800 °C to a value of Kp = 8.6×10^{-7} ($mg^2/cm^4.s$) at 1000 °Cand (Q= 187.6 kJ/mol), and for NiTi 0.9 wt.% Y, (kP) differs from a value of kP = 1.0780×10^{-7} ($mg^2/cm^4.s$) at 800 °C to a value of kP = 7.2531×10^{-7} ($mg^2/cm^4.s$) at 1000 °C. and Q =123.98 kJ/mol. The phases presented after periodic oxidation at 1000 °C for 100 hrs. and 10 hrs. per period of NiTi 0.9%Y SMA surface as revealed by XRD analysis were NiTi monoclinic, NiTi cubic, Ni_3Ti, and TiO_2

KEYWORDS: NiTi, Shape Memory Alloy, Oxidation, Yttrium & Activation Energy

Received: Mar 10, 2020; **Accepted**: Mar 30, 2020; **Published**: Apr 08, 2020; **Paper Id**.: IJMPERDAPR202011

1. INTRODUCTION

Nitinol has quickly become the most suitable material for selection for numerous implantation instruments, like self-expanding stents, according to its superelasticity characteristics. Though numerous research have confirmed decent resistant of corrosion as well as biocompatibility that Nitinol offers **[1-3],** current research have revealed that in certain suitcases Nitinol implants could be corroded in vivo and release of great content of nickel [4, 5]. It is accepted that the corrosion resistant of Nitinol alloy can be appropriately enhanced by modification of the surface like electro-polishing [1]. Electro-polishing of Nitinol creates a protector regular TiO_2 scale which defends the substrate metal from corroded environments. At high temperature air environments, Ti interact with oxygen gas to create a titanium oxide scale, besides the structure of TiO_2 scale is appropriate taking into consideration the bio-compatibility of materials. At the same time, many Nitinol implants have undergone many thermal periods to shape-set the apparatuses or adjust their transformations temperatures as the last surface improvements techniques, in addition, it's appropriate to estimate the influences of Nitinol high temperature oxidation on its resistance against

corrosion. Many authors [6-12] inspected the influences of surface modifications on the NiTi surface constituents; however, the oxidation mechanism at elevated temperature is not entirely realized.

NiTi-base Shape-Memory Alloys (SMAs) are the greatest significant SMAs owing to their greater qualities in the effect of shape-memory (SME), damping capacity and pseudoelasticity **[13]**. It was prevalent that the adding of an additional element could change the mechanical properties of binary NiTi alloys and their phase transformation behavior **[14]**. Ti50Ni50-xYx alloys have concerned much consideration in SMAs' demands in which the SMAs are typically manufactured to a plate form or wire. The fabrication procedures of SMA wire or plate are wiredrawn or hot-rolled, and both were manufactured at elevated temperature scales on the external surface. Accordingly, a comprehension of the elevated temperature scales consistence on the NiTi based SMAs is required, and the performance of oxidation of NiTi SMA was explored by some investigators **[15–19]**. The apparent activation energy (Q) for the oxidation reaction of Ni50Ti50 SMA was equal to 226 kJ/mol, and the oxidation rate exhibits a parabolic relationship **[17]**. A multiple layered of oxide scale was consistence on Ti50Ni50 SMA, comprising of an outer scale of TiO_2, a porous intermediate scale of the combination of Ni(Ti), TiO_2 and a thin inner scale of $TiNi_3$ **[17]**.

Oxidation resistant progress by adding designated alloying elements [20], several investigators elaborated in this field and they considered the adding consequence of alloying elements such as chromium, copper and aluminum into alloys of nitinol and studied its effect the performance of nitinol SMAs in high temperatures and corrosive surroundings [21,22]. K. N. Lin et al. [21] examined the iso-thermal oxidation performance of Ti50Ni40Cu10 (SMA) in 700 to 1000 ℃ static air, whereas, James and Smialek [23] investigated the oxidation behavior of an elevated temperature shape memory alloys, Ni30Pt50Ti (at.%) by isothermal oxidation in static air for 100 hrs at limited temperature variety from 500 to 900 ℃. In addition to that, Kim et al. [24] investigated the hafnium addition influence on the oxidation behavior and the Ti-49Ni-12Hf oxide structure and the SMAs at elevated temperatures. In the current work, the influence of adding various Yttrium contents (0.5 and 0.9 wt%) was investigated. To the best authors' knowledge, the oxidation behavior and mechanism of NiTiY SMAs are not systematically studied yet. In this work, NiTiY SMA was oxidized at elevated air temperature. The mechanism of oxidation and the activation energy are conversed and compared with those of binary NiTi.

2. EXPERIMENTAL WORK

2.1. Materials Used

Ni, Ti and Y powders were used in this work to manufacture specimens in this work.

2.1.1 Powders

The powders' specifications are listed in Table 1 along with the percentage of purity and average size of the particles (µm).

Table 1: Powders used to Produce NiTi Specimens

Materials	Purity %	Average size of particles (µm)
Titanium powder	99.86%	13
Nickel powder	99.21%	29
Yttrium powder	99.99%	8.5

2.1.2 Manufactured of Specimens

Powder metallurgy technique (P. M.) is used to manufacture specimens of nitinol SMAs. The procedure includes blending, compressing and sintering technique. Table 2 comprise the alloys constituents used in the current study.

Table 2: The Constituents of the Manufactured Alloys in Weight Percentage

Alloys No.	Chemical Composition Weight Percentage
1	55 Ni - 45Ti
2	54.5 Ni - 45Ti – 0.5 Y
3	54.1 Ni - 45Ti –0.9 Y

2.1.3 Blending of Powders

Nickel and Titanium powders with Yttrium as modifiers were limited in accordance with the required amounts. Wet blending was done using an electrical rolling blender instrument to get a uniform powder dispersion. Ceramic balls having various diameters were utilized through the blending process to settle blending the powder for five hours. Ethyl alcohol was supplemented for preventing the friction between the powder particulates and the walls of the mold and reducing the particulates oxidation through blending procedure.

2.1.4 Powders Compressing

Steel die with cylindrical shape was employed to manufacture the specimens by compressing pressure (800 MPa). The applied compacting pressure was done via an electric hydraulic press. Graphite as emollient was supplemented in tiny amounts to minimize the friction developed between particulates and die walls through compressing.

2.2 The procedure of Sintering

The green compressed specimens were subjected to sintering procedure using a tube oven with quartz pipe and vacuum pumps where it can get a vacuum atmosphere up to (10^{-4}) tor. The procedure was illustrated in Figure1. When the sintering procedure was completed, the specimens were kept in the oven to cool down up to room temperature.
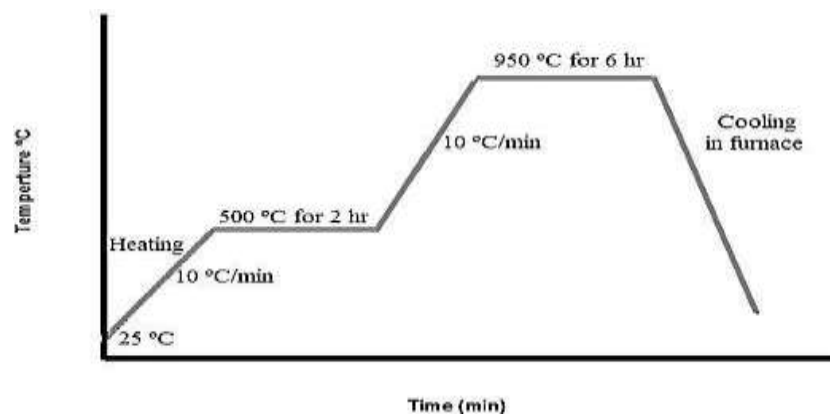
Figure 1: Sintering Procedure of Compressed Specimens.

2.3 Manufacturing of Specimens for Tests

All specimens after finishing sintering procedure were subjected to grinding utilizing (180, 320, 600, 800, 1000,1200, and 2000) grit silicon carbide cloth, then refined with a past of diamond (0.3 μm) to obtain a satin mirror surface for the last stage. The etching process was done using the following etching solution illustrated in Table 3, was done at 25 ℃. Later, the specimens were scavenged and rinsed by water and then carefully dried.

Table 3: The Chemical Compositions and
Concentrations of the used Etchant Solutions [25]

Chemical composition	Etchant Concentration (%)
$HNO_3 + HF + H_2O$	20% + 10% + 70%

2.4. Measuring of Porosity and Density

Densities and porosities before and after sintering were determined according to the following sections.

2.4.1 Measuring of Green Porosity and Green Density

Green density can be defined as a unit volume weight of compressed mixed powder determined g/cm^3. It is determined from measure of weight and dimensions of the compressed specimen as the following **[26]**:

$$\rho_g = \frac{m_g}{V_g}$$

(1)

Where:

ρ_g = green density (g/cm^3). , m_g = green mass of the compact (g).

V_g = volume of the compact (cm^3).

The green porosity can be calculated from the blending theoretical density that is considered by the percentage weight of individual powders multiplies by their theoretical densities as the following **[26]**:

$$\dot{p}_{tB} = \sum_{i=1}^{n} Wt_1 * \rho_1 + Wt_2 * \rho_2 + Wt_3 * \rho_3 + \ldots + Wt_n * \rho_n$$

(2)

where:

ρ_{tB} = theoretical density of blended powder (g/cm^3). , n = No. of elemental powders.

W_t = weight percent (%),

$\rho_{1\ldots n}$ = density of elemental powder (g/cm^3).

therefore, the green porosities can be calculated using the next equation **[26]**:

$$P_g = \left(1 - \frac{\rho_g}{\rho_{tB}}\right) \times 100\%$$

(3)

where

P_g = green porosity (%) . ρ_g = green density (g/cm^3).

ρ_{tB} = theoretical density of blended mixture (g/cm^3).

True Porosities for Sintered specimens

2.4.2 Measuring of True Porosity for Sintered Specimens

Measuring of True Porosity for Sintered Specimens can be done according to ASTM B-328 as the following steps[27]:

- The specimens are dried at 100 °C for 5hrs. in vacuum condition at (10^{-4}) tor then cooled to R.T. by vacuum dryer oven. The dry specimen weight is symbolized as a mass A.

- At R.T., by a sufficient vacuum pump. The pressure had been decreased to the immersed sample in a suitable oil for 0.5 hr.

- Weighting the entirely impregnated specimens in air, and is symbolized as mass B.

- Weighting the completely impregnated specimens in water, and is symbolized as mass F.

- Lastly, the porosity was calculated by the equation below:

$$P = \left[\frac{B-A}{(B-F)D^\circ} \times 100 \right] Dw$$

(4)

Where:

D_w= water density (0.9956 g/cm3)

D_0 =oil density (0.8 g/cm3)

2.5 Inspection of Microstructure Using Scanning Electron Microscope (SEM)

The specimens' microstructures were inspected after sintering procedure by Scanning Electron Microscope (SEM).

2.5.1 Periodic Oxidation

Periodic oxidation at elevated temperature (800, 900, and 1000 °C) were done to investigate the oxidation behavior and the influence of yttrium additive on oxidation performance evaluation of NiTi (SMAs). Through periodic oxidation, the temperature of oven was regulated by including± 3℃. All NiTi alloys specimens without and with (0.5%, 0.9%) wt.% yttrium are tested. In each period, the specimens are pulled outside the oven to cool in the static air immediately after the heating period ends, and so the rest of the thermal periods are repeated until it reaches 100 hrs. Specimens weight recorded before and after each oxidation period.

2.6 X- Ray Diffraction Analysis

X-ray diffraction analysis was done for the powders of (Ni, Ti and yttrium) individually for each specimen after sintering and after the end of periodic oxidation tests. The XRD generator having Cu target at 30 mA and 40 KV, scanning speed 5 degree/min was performed. The range of scanning was (10° – 90°).

3. RESULTS & DISCUSSIONS

3.1 Influence of Compacting Pressure and Sintering Procedure on Density and Porosity

Numerous compacting pressures (600, 700 and 800) MPa were utilized in manufacturing the compressed specimens. Figure 2 exhibits the Ni-Ti specimens' densities with and without adding yttrium (0.5, 0.9) wt.%. When increasing the

Pressure of compacting, the green density increased similarly till it extents a definite value where any additional growth in the applied pressure load has no or a small influence on its rate. Consequently, the favored pressure was equal to 800 MPa for all manufactured specimens.
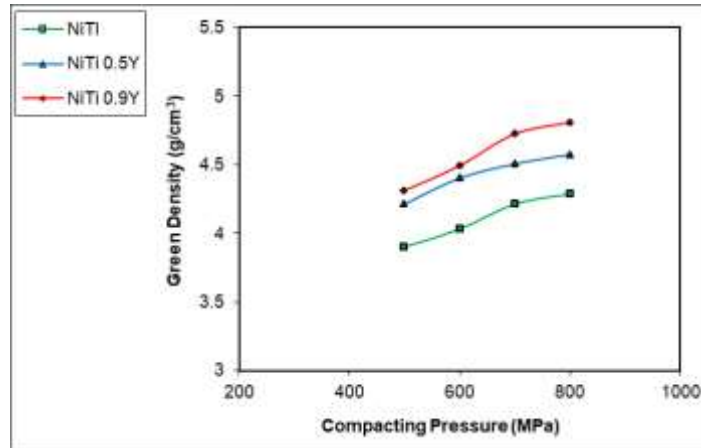
**Figure 2: Green Density vs. Compacting Pressure prior the Sintering
Procedure of NiTi Alloy without and with Various Amounts of Yttrium.**

The outcomes in Figure 3 display the specimens of NiTi with and without adding yttrium after sintering process. It illustrates that the density increased continuously as in Figure 2. This can be attributed to the sintering procedure (950 °C for 6 hrs.) that cause increasing diffusion and reduction in voids. Since the particle size of the element yttrium is less than the particle size of nickel and titanium, this means an increase in contact points between the blended powder particles. Moreover, increasing yttrium content can increase the density. These results are in agreement with Nawal et. al.**[28].**
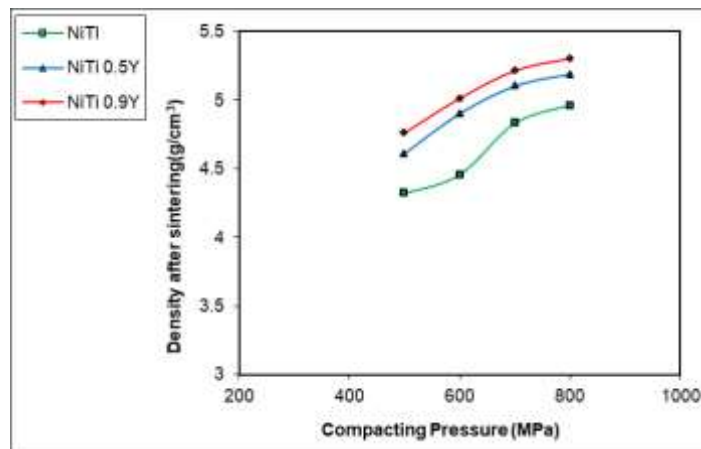
**Figure 3: Density vs. Compacting Pressure after Sintering Procedure (at 950 °Cfor 6hrs.)
of NiTi Alloy without and with Yttrium.**

Figure 4 shows that increasing in the compact pressure give rise to a reduction in the green porosity owing to increasing the contact points between particulates that minimize voids.
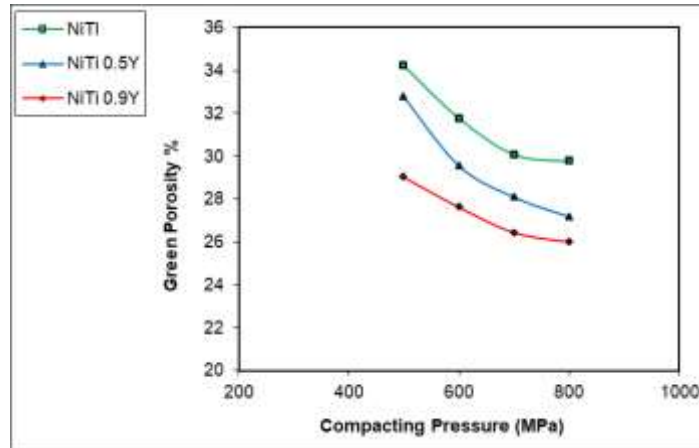
**Figure 4: Green Porosity vs. Compacting Pressure before Sintering
Procedure of NiTi Alloy without and with Yttrium.**

The outcomes in Figure 5 display the specimens' porosity after sintering procedure. It demonstrates that the porosity can be reduced owing to the sintering at 950 °C for 6 hrs. This can increase the diffusion between particles that decrease the voids content and in turn increase the contacted points between particles. This parameter would minimize the porosity.

3.2 Effects of Y Contents on Density and Porosity after Sintering:

Figure 6 demonstrates the yttrium influence on sintered specimen's porosity. The porosity of specimens decreased after sintering procedure. Porosity decreased as Y additions increased due to the particle sizes of Y is lower than that of Ti or Ni; therefore, when it occupies the interstitials positions, the porosity decreased.
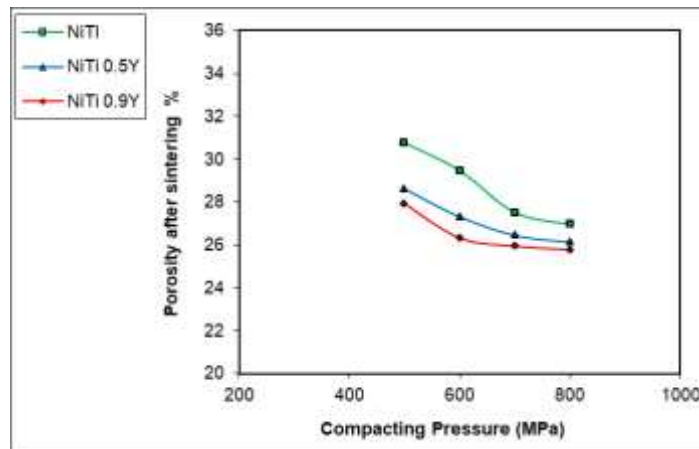
**Figure 5: Porosity vs. Compacting Pressure after Sintering Procedure (at 950°C for 6hrs.)
of NiTi Alloy without and with Yttrium Amount.**
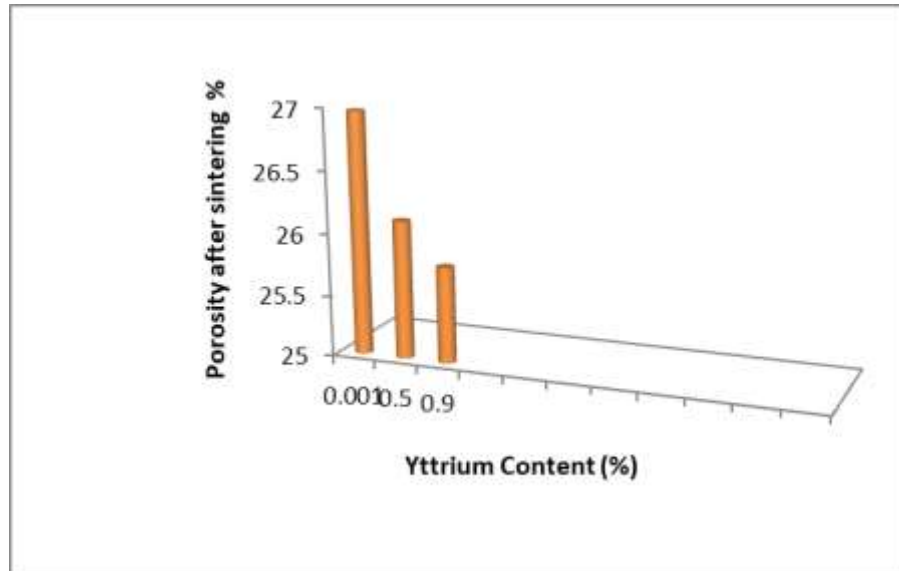
**Figure 6: Influences of Yttrium amount on Porosity afterward
Sintering Procedure for NiTi Alloy.**

3.3 Scanning Electron Microscopy

The microstructures arrived from SEM for specimens without and with (0.9 wt.% Y) adding after being etched were revealed in Figures 7 and 8, correspondingly. As an outcome, the sintered specimen microstructure displayed a multi- phase construction whereas the two phases [B2 (NiTi Cubic-phase) and B19′ (NiTi monoclinic phase)]; therefore, validating the XRD results.

Figures 7 and 8 show that etching can reveal the boundaries of the grain, that easily distinguish with the boundaries of grains and pores form. The martensite shaped in entirely alloys had needle formed grains. The order or dis-order of the parental phase B2 was converted to martensite, taking into consideration disorder B2 forms disordered martensite **[29].**
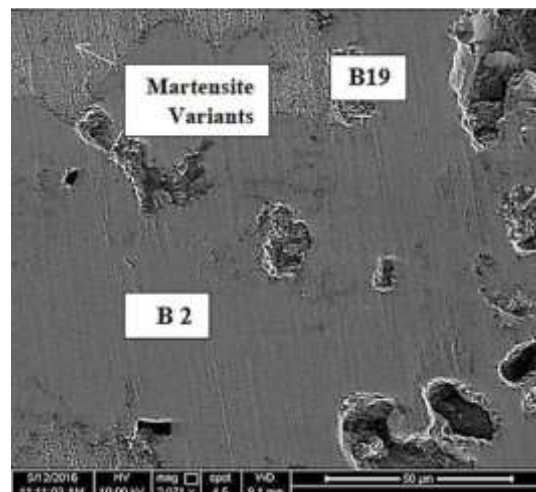
Figure 7: SEM of NiTi Alloy.
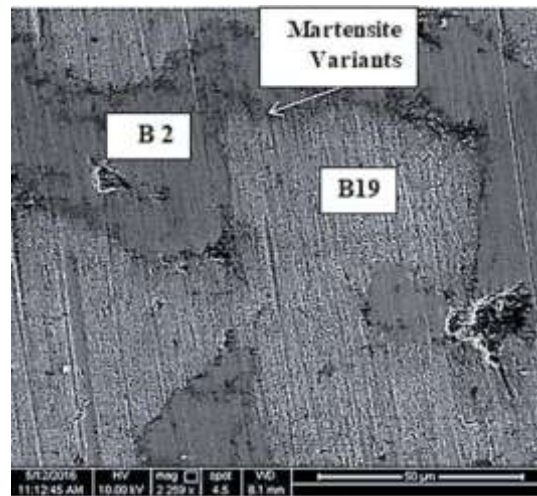
Figure 8: SEM of NiTi +0.9%Y Alloy.

3.4 Periodic Oxidation

This paragraph explains over the behavior of oxidation of NiTi (SMAs) and the influence of yttrium on these behaviors. NiTi specimen with chemical composition of (45% Ti and 55% Ni,) was examined to supply a typical to be associated with alloys periodic oxidation resistant that comprise of (0.5% and 0.9%) Yttrium. The function of Yttrium in modifying periodic oxidation resistant will be clarified. Gaining of weights were documented for kinetics definition in dried atmosphere in the temperature variety 800 –1000 °C for 100 hrs. and 10 hours per period. Data of gain of specific weight of alloys and NiTi comprise (0.5% and 0.9%) yttrium for every temperature test is schemed as a time function.

$$\Delta W/A = kt^n \tag{5}$$

Whereas (ΔW) denotes the gain of weight, (A) denotes the tested specimen surface area, (t) is the oxidation time, (k) denotes a factor related to rate constant, (n) denotes the time constant-growth-rate.

3.5 NiTi Alloy Oxidation

The n-rate of NiTi alloy at 800 °C is around (0.49) i.e., the performance is parabolic and it is found by (A computer database is employed to determine values of n by virtue of the Equation (5) best fit to Additional n values for entirely specimens at different values of temperatures are revealed in Table4. Figure 9 presented parabolic-fitted outcomes of gain of weight with respect to time. scheme for NiTi alloy periodic oxidized in dry air between 800 and 1000 °C for 100 hrs. and 10 hours per period. These outcomes display that at these temperature, the parabolic kinetics can be calculated using enhanced law of a parabolic rate with the supposition that oxidation is measured by mechanisms of diffusion and the boundaries of grains are the solitary active diffusion tracks of short circuit [30].
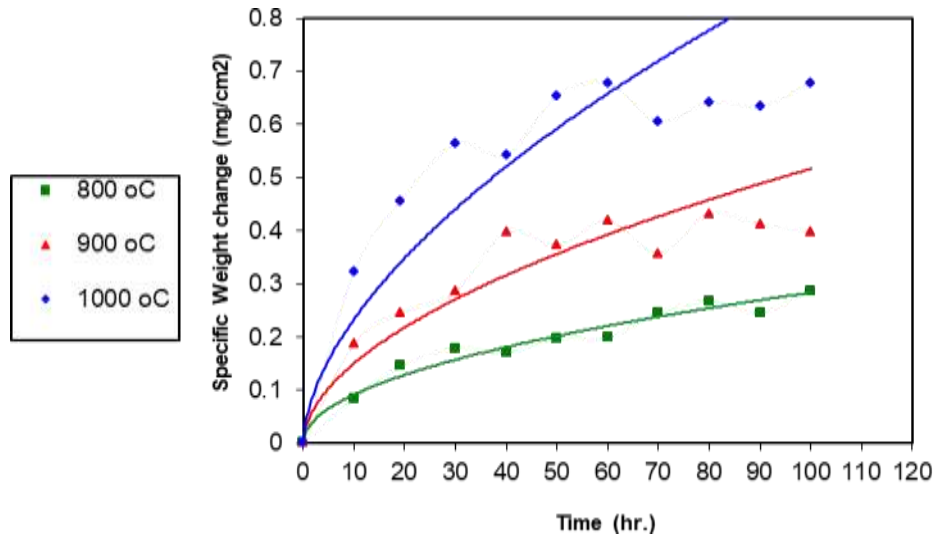
Figure 9: Fitted Parabolic Results of Specific Weight Gain with Respect to Time for NiTi Alloy Periodic Oxidized in air at different temperatures for 100 hrs and 10 hours per period.

As per parabolic kinetics, the rate equation receipts the formula:

$$\Delta W/A = kt^{0.5} \tag{6}$$

The letter k denotes the constant of parabolic rate. Figure 10 shows the relationship between the gain of the specific weight as function for the time square root that provides a line as illustrated; the sloping is the constant of the parabolic rate measured by $(mg/cm^2)/hr.^{1/2}$. This squared to obtain kP in units of $(mg^2/cm^4)/hr..$, as shown in the subsequent expression:

$$(\Delta W/A)^2 = kPt \tag{7}$$
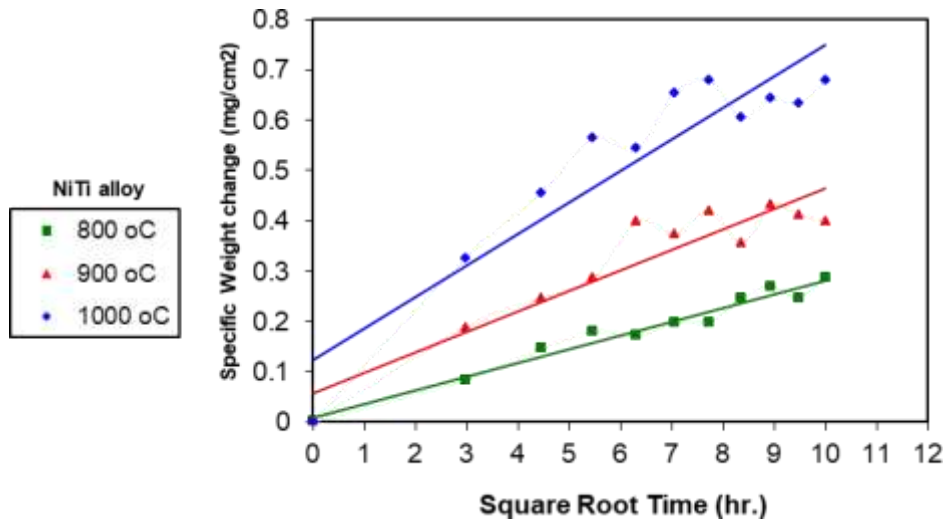
Figure 10: Linearly Fitted outcomes of Gain of Specific Weight vs. t $^{0.5}$ scheme for NiTi For Periodic Air-Oxidized among 800 and 1000 °C for 100 hrs. and 10 hours per Period

The constants of parabolic oxidation rate for three trials sequences are determined. The straight lines indicate the curve fits (least squares) to the values of data in Figure (11), The constants of the parabolic oxidation rate (kP) for the set of

experiments are itemized in Table (4).
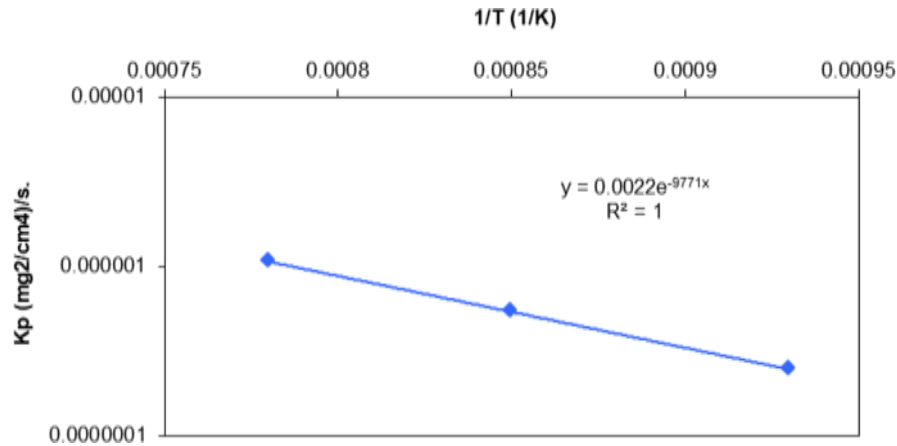
Figure 11: Scheme of kP vs. 1/T for Periodic Oxidized of NiTi Alloy in Air for 100 hrs and 10 hours per Period.

Table 4: n Values and Rate Constants of Parabolic Oxidation kP for NiTi alloy Periodic Oxidation in air for 100 hrs. and 10 hours per Period

Temperature (°C)	n values	Kp (mg^2/cm^4.s)
800	0.49	2.4502 x10^{-7}
900	0.53	5.3534 x10^{-7}
1000	0.57	10.609 x10^{-7}

At the range of temperatures from 800-1000 °C, the rate coefficients of parabolic oxidation and accordingly the oxidation rates of of NiTi alloy in air, differ in amount from 2.4502×10^{-7} (mg^2/cm^4.s) at 800 °C to a higher value of 10.609×10^{-7} (mg^2/cm^4.s) at 1000 °C. The fact to be seen is that the gain in weight determined by submission of the rates coefficient of parabolic oxidation in Table 4 with Equation no. 3 produced in the weight of oxygen increased by the specimen underneath period of oxidation. Also, the insights to be seen, is that the additional values of kP and n in this investigation are determined with the similar method discussed above. Consequently, data exhibited that a parabolic oxidation rates (kP) follows an equation of Arrhenius-type as:

kP =ko exp(-Q/RT)   (8)

where kP is the rate of parabolical oxidation, ko is the pre-exponential factor, Q is the activation energy, and R is the gas constant (8.33 J/K) [**31**], and T is the temperature. Draw of log (kP) vs. (1/T), the operative energy is determined from the fitting of least square (R^2 = 1) of the seen data in the range from 800 to 1000 , which is approximately equal to 297 KJ/mol. as illustrated in Figure 11. The obtained value is in a good agreement with the data from James L. Smialek [**23**].

3.6 Oxidation of (NiTi0.5Y) and (NiTi0.9Y) Alloy

It is to be noted from Figures 12 to 15 that the behavior of the two alloys (NiTi 0.5Y) and (NiTi 0.9Y) follows parabolic behavior when oxidized in a periodical manner in air for 100 hrs. and 10 hrs. per period and as it is noticed that the rise in temperature leads to an increase in weight as well.
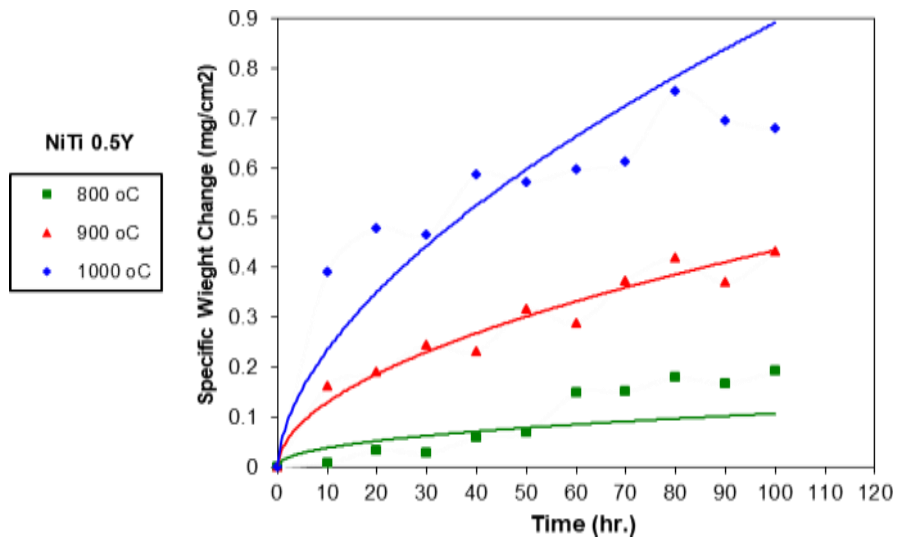
**Figure 12: Fitted-Parabolic Results of Gain of the Specific Weight vs. Time Scheme
for Oxidized NiTi 0.5%Y Alloy Periodic in Air among
800 and 1000 °Cfor 100 hrs. and 10 hrs. per Period.**
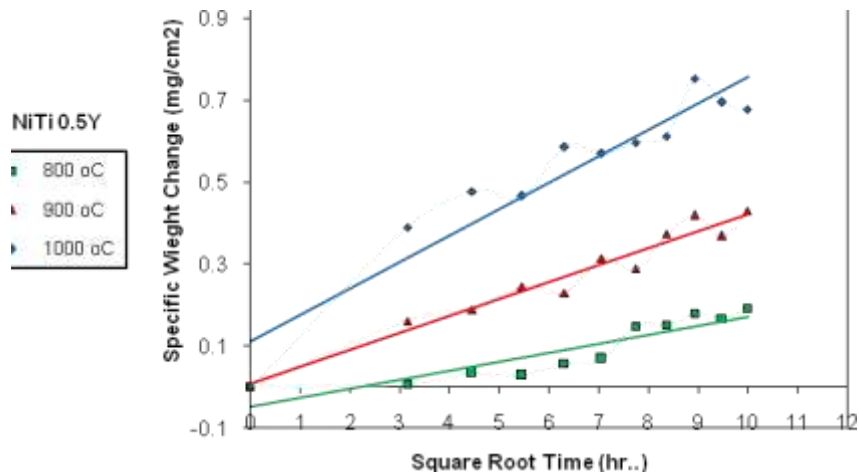
**Figure 13: Fitted-Linear Results of Gain of the Specific Weight vs. t$^{0.5}$ Scheme for
Oxidized NiTi 0.5Y Alloy Periodic in Air among 800 and 1000 °C
for 100 hrs. and 10 hrs. per Period**
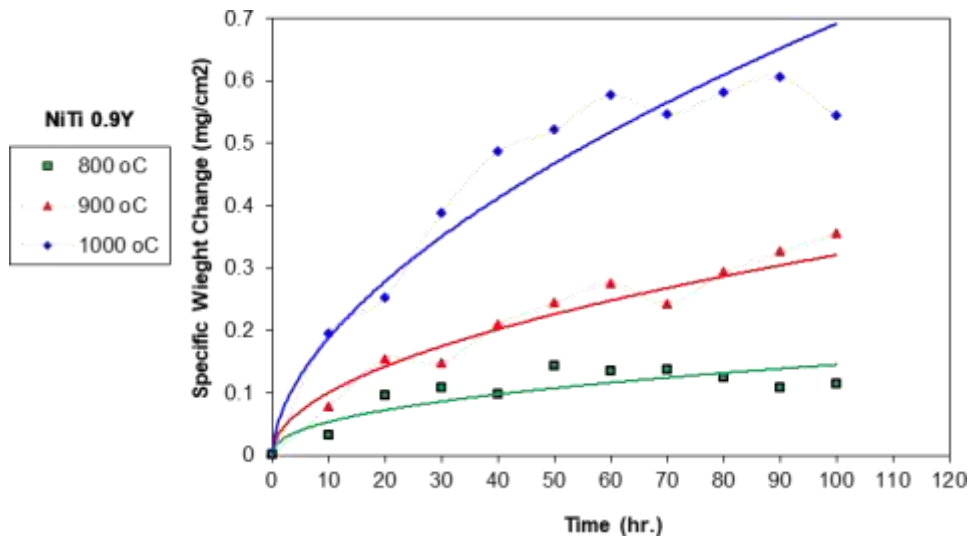
Figure 14: Fitted-Parabolic Results of Gain of Specific Weight vs. Time Scheme
for Oxidized NiTi 0.9%Y Alloy Periodic in Air among 800 and 1000 °C for 100 hrs. and
10 hrs. per Period.
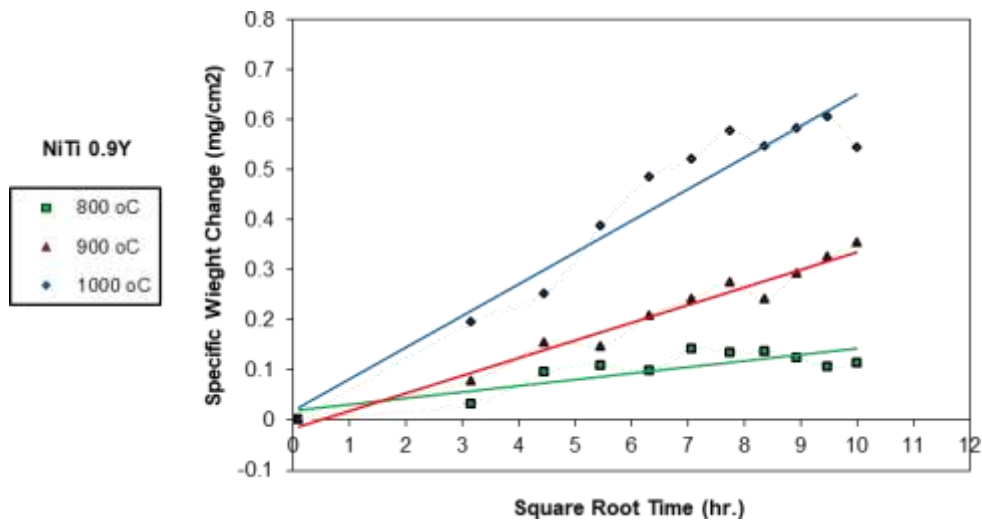
Figure 15: Fitted-Linear Results of Gain Specific Weight vs. $t^{0.5}$ Scheme for Oxidized
NiTi Alloy Periodic in air among 800 and 1000 °C
for 100 hrs. and 10 hrs. per Period.

From the experimental data, the (kP) log with respect to (1/T) is schemed in Figures16 and 17, (n, kp, and Q) revealed in Table 5 were determined from least square fitting of the recorded information in the range of temperature from 800 to 1000 ℃.
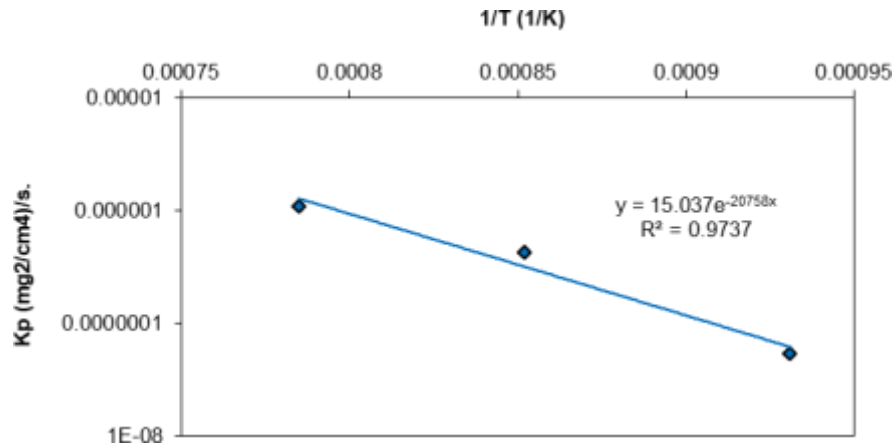
**Figure 16: Scheme of kP vs. 1/T for Oxidized NiTi 0.5 Y
Alloy Periodic in Air for 100 hrs. and 10 hrs. per
Period**
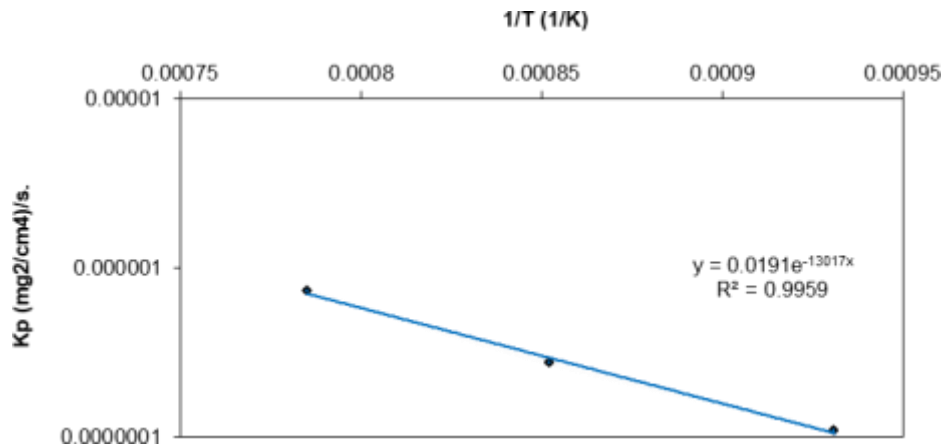
**Figure 17: Scheme of kP vs. 1/T for Oxidized NiTi 0.9 Alloy Periodic
in air for 100 hrs. and 10 Hours per Period.**

**Table 5: values of (n),(kP), and (Q)for (NiTi 0.5% Y) and (NiTi 0.9% Y) alloy periodic
oxidized in air for 100 hrs. and 10 hours per period**

alloy	Temperature (°C)	n values	kP(mg²/cm⁴.s)	Activation energy kJ/mol
NiTi 0.5% Y	800	0.443	0.536×10^{-7}	
	900	0.524	4.185×10^{-7}	187.6
	1000	0.577	10.754×10^{-7}	
NiTi 0.9% Y	800	0.433	1.078×10^{-7}	
	900	0.5053	2.721×10^{-7}	123.95
	1000	0.5657	7.253×10^{-7}	

outcomes established that gain in weight affected by the quantity of yttrium additional to the alloy. At 800°C, gain

in weight of alloy that comprises(0.9%Y) is lesser than the others, therefore, the resistance of oxidation is the

maximum since the oxide scale thickness is lesser. Which means that oxide scale create on the surface of metal could stop more reactions with oxygen at(900and 1000)°C oxidation resistant is the upper most at(0.9%Y).

3.7 X- Ray Diffraction Tests

Figures 18 demonstrate the XRD configuration for NiTi with the 0.9Y addition afterward sintering procedure. It can be realized that Ti and Ni converted to (B2 austenite and B19 martensite). This illustrates that the procedure time of sintering (6 hrs. at 950 °C) was sufficient to complete the phases alteration procedures. The nonappearance of pure elements are important in the X-ray diffraction analysis is very important. If we consider the toxicity caused due to some pure elements biomaterials applications. Yttrium compounds have not been clearly demonstrated in the X-ray diagrams, and this is due to the low-level added yttrium (0.9), which is outside the limits of the possible detection ranges.
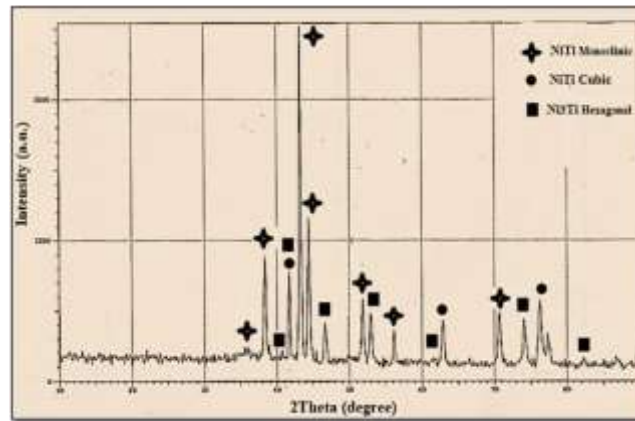
Figure 18: XRD Configuration for NiTi0.9%Yalloy afterward Sintering Procedure.

Figure19 demonstrates XRD configurations of NiTi 0.9%Y alloy after subjected to periodic oxidation at 1000 °C. Oxides are created on the specimen surface. The main constituent of these oxides is titanium oxide. That means that TiO_2 development controls the oxidation behavior. This is due to the action of yttrium or yttrium compounds phases which may be found on the outer scale in small amounts [32].
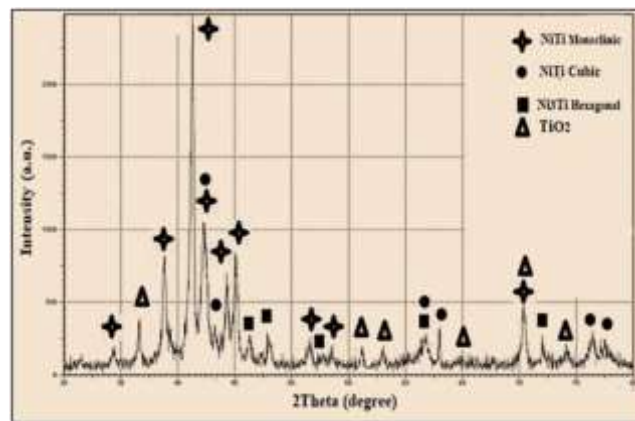
**Figure 14: XRD Configurations of NiTi 0.9%Y SMA after Periodic Oxidized
for 100 hrs and 10 hours per Period at 1000 °C.**

4. CONCLUSIONS

- Procedure of sintering procedure at 950 °C for six hours (with and without yttrium addition) is sufficient to fulfillment the process of transformation of nickel, titanium and yttrium to alloy construction.

- The results of scanning electron microscopy showed that the main phase formed for all specimens without and with the addition of yttrium the martensite phase.

- The porosity decreases significantly with the addition of yttrium.

- The X-ray examination results indicated formation of austenite (B2) and monoclinic NiTi (B19) for all specimens.

- The NiTi alloy showed good periodic oxidation resistance at temperatures 800 °C, 900°C and 1000 °C.

- Alloy of the NiTi showed satisfactory resistance for periodic oxidation at 800 , 900 and 1000 °C, respectively.

- The addition of yttrium to the NiTi alloy greatly improved the oxidation resistance in general, and the addition 0.9 wt.% Y gave the best results in particular.

- All NiTi alloys (without and with additives) showed parabolic oxidation response in all conditions.

- The energy of activation of NiTi is ~ 297 kJ/mol,(NiTi0.5%Y)~ 187.6 kJ/mol and that for (NiTi0.9%Y) ~ 123.95 kJ/mol. This is a very clear indication of the low activation energy to form a protective layer of titanium oxide with the addition of yttrium to the nickel titanium alloy.

REFERENCES

1.   *L. Zhu, C. Trépanier, A. R. Pelton and J. Fino, Oxidation of Nitinol and its Effect on Corrosion Resistance, ASM Materials & Processes for Medical Device Conference,2003.*

2.   *G. S. Firstov*, R. G. Vitchev1, H. Kumar, B. Blanpain, J. Van Humbeeck, Surface oxidation of NiTi shape memory alloy, Biomaterials 23 (2002) 4863–4871.*

3.   *Abdus Mahmuda, b, Zhigang Wua, c,∗∗, Junsong Zhanga, Yinong Liua,∗, Hong Yanga, Surface oxidation of NiTi and its effects on thermal and mechanical properties,Intermetallics103(2018)52–62.*

4.   *A. Michiardi, C. Aparicio, J. A. Planell, F. J. Gil, New Oxidation Treatment of NiTi Shape Memory Alloys to Obtain Ni-Free Surfaces and to Improve Biocompatibility, MICHIARDI ET, AL Wiley InterScience (www.interscience.wiley.com). DOI: 10.1002/jbm.b.30441, 2005, pp.249-256.*

5.   *N. M. Dawood, A. K. Abid Ali, and A. A. Atiyah, Fabrication of Porous NiTi Shape Memory Alloy Objects by Powder Metallurgy for Biomedical Applications, IOP Conf. Series: Materials Science and Engineering, 518 (2019) 032056, doi:10.1088/1757-899X/518/3/032056*

6.   *M. Duerig and P. Sinclair, Two-Step Martensitic Transformations in TiNi (10% Cu) Shape Memory Alloy, Materials Research Society Symposium Proceedings Vol. 245 "Shape Memory Materials and Phenomena - Fundamental Aspects and Applications" 1992, pp. 55-60*

7.   *Z. Yang, X. Wei, P. Caoand W. Gao, Surface Modification of Nitinol by Chemical and Electrochemical Etching, Modern Physics Letters B, Vol. 27, No. 19, (2013) 1341012 (7 pages).*

8.   *F. Sun , K. Sask, J. Brash, I. Zhitomirsky, Surface Modifications of Nitinol for Biomedical Applications. Colloids Surf B Bio interfaces. 2008 Nov 15;67(1):132-9. doi: 10.1016/j.colsurfb.2008.08.008. Epub 2008 Aug 22.*

9.   *Z. Yang, X. Wel, P. Cao and W. Gao, Surface Modification of Nitinol by Chemical and Electrochemical Etching, Modern Physics Letters B, Vol. 27, No. 19, 1341012 (2013)*

10.   *O. A. Kashin, D. P. Borisov, A. I. Lotkov, P. V. Abramova, and A. V. Korshunov, Influence of surface modification of nitinol*

with silicon using plasma-immersion ion implantation on the alloy corrosion resistance in artificial physiological solutions, AIP Conference Proceedings 1683, 020077 (2015); https://doi.org/10.1063/1.4932767S. Trigwell, et al., in Sufr Interface Anal, 26, 1998, p. 483-489.

11. *S. Shabalovskaya, J. Anderegg, J. Van Humbeeck, Critical overview of Nitinol surfaces and their modifications for medical applications, ActaBiomaterialia 4 (2008) 447–467.*

12. *A F Mansor, R Jamaluddin, A I Azmi, T C Lih and M Z M Zain, Surface modification of nitinol by using electrical discharge coatings in deionized water, IOP Conf. Series: Materials Science and Engineering 670 (2019) 012010, doi:10.1088/1757-899X/670/1/012010C.*

13. *Xiangmei Liu, Shuilin Wu, Y. L. Chan, Paul K. Chu, C. Y. Chung, C. L. Chu, K. W. K. Yeung, W. W. Lu, K. M. C. Cheung, K. D. K. Luk, Structure and wear properties of NiTi modified by nitrogen plasma immersion ion implantation, Materials Science and Engineering A 444 (2007) 192–197*

14. *Xiangqing Kong, R. G. Grabitz, W. van Oeveren, D. Klee, T. G. van Kooten, F. Freudenthal, Ma Qing, G. von Bernuth, M.-C. Seghaye, Effect of biologically active coating on biocompatibility of Nitinol devices designed for the closure of intra-atrial communications, Biomaterials 23 (2002) 1775–1783*

15. *F. S. Hameed and A. H. Haleem, Investigation the Effects of Germanium addition on the Oxidation Behavior of NiTi shape memory Alloy in Air, ADVANCES in NATURAL and APPLIED SCIENCES, 2017 January 11(1): pp. 31-44.*

16. *Edin Bazochaharbakhsh, Surface Nitriding and Oxidation of Nitinol, Master's Theses, San Jose State University,August 2011.*

17. *S. A. Shabalovskaya, H. Tian, J. W. Anderegg, D. U. Schryvers, W. U. Carroll and J. V. Humbeeck, "The Influence of Surface Oxides on the Distribution and Release of Nickel From Nitinol Wires," Biomaterials, 30, 468-477,(2009).*

18. *G. S. Firstov, R. G. Vitchev, H. Kumar, B. Blanpain and J. Van Humbeeck, "Surface Oxidation of NiTi Shape Memory Alloy," Biomaterials, 23(24), 4863-4871(2002).*

19. *L. Zhu, J. M. Fino and A. R. Pelton, "Oxidation of Nitinol," in International Conference on Shape Memory and Superelastic Technologies, USA, 2003, pp. 357–368, (2003).*

20. *D. Mudgal, S. Singh and S. Prakash, "High Temperature Periodic Oxidation Behavior of Ni and Co Based Super alloys", Journal of Minerals & Materials Characterization & Engineering, Vol. 11, No.3, pp.211-219, (2012).*

21. *K. Lin and Sh. Wu, "Oxidation Behavior of Ti50Ni40Cu10 Shape-Memory Alloy in 700–1,000 _C Air", Oxid. Met, Taiwan, P. 187–200 (2009).*

22. *C. Craciunescu and A. S. Hamdy, "The Effect of Copper Alloying Element on the Corrosion Characteristics of Ti-Ni and Ternary Ni-Ti-Cu Meltspun Shape Memory Alloy Ribbons in 0.9% NaCl Solution", Int. J. Electr°Chem. Sci, Egypt No.8, P. 10320 - 10334 (2013).*

23. *J. L. Smialek, D. L. Humphrey and R. D. Noebe, "Comparative oxidation kinetics of a NiPtTi high temperature shape memory alloy", Oxidation of metals, P. 125-144. (2010).*

24. *K. M. Kim, J. T. Yeom, H. S. Lee, S. Y. Yoon and J. H. Kim, "High temperature oxidation behavior of Ti–Ni–Hf shape memory alloy". Therm°ChimicaActa, 583, 1-7. (2014).*

25. *P. Walker and W. H Tarn, "CRC handbook of metal etchants", CRC press, (1990).*

26. *S. A. Ajeel, A. K. A. Ali and M. A. Alher, "Ni Ion Release of TiO2 and TiO2/Hydroxylapatite composite coatings formed on NiTi shape memoryalloy produced by powder metallurgy". International Journal of Mechanical Engineering and Technology, P. 86-99, (2013).*

27. *ASTM B-328" Standard Test Method for Density, Oil Content, and Interconnected Porosity of Sintered Metal Structural Part and Oil – Impregnated Bearing "ASTM international, 2003*

28. *Atiyah, A. K. Abid Ali, N. M. Dawood, Characterization of NiTi and NiTiCu Porous Shape Memory Alloys Prepared by Powder Metallurgy (Part I), Arabian Journal for Science and Engineering, 40, pp.901–913(2015)*

29. *N. M. Dawood, " Preparation And Characterization Of Bio Nitinol With Addition Of Copper", PhD. thesis, materials engineering department, university of technology/ Iraq, 2014.*

30. *Michiardi, C. Aparicio, J. A. Planell and F. J. Gil, "New Oxidation Treatment of NiTi Shape Memory Alloys to Obtain Ni-free Surfaces and to Improve Biocompatibility," J. Biomed. Mater. Res., 77, pp.249-256, 2006.*

31. *D. Vojtech, P. Novak, M. Novak, L. Joska, T. Fabian, J. Maixner and V. Machovic, "Cyclic and Isothermal Oxidations of Nitinol Wire at Moderate Temperatures," Intermetallics, 16, 424-31, (2008).*

32. *A. H. Khilfa"Effect of Y and Ge addition on Mechanical properties and Corrosion Behavior of Biomedical C°CrMoAlloy (F75)", master thesis, Materials engineering, University of Babylon, (2015).*